Wave Loads on a Point-Absorbing Wave Energy Device in Extreme Waves

Malin Göteman[a], Jens Engström[a], Mikael Eriksson[a,d], Martyn Hann[b], Edward Ransley[b], Deborah Greaves[b], Mats Leijon[a,c,d]

[a]Department of Engineering Sciences, Uppsala University, Uppsala, Sweden

[b]School of Marine Science and Engineering, Plymouth University, Plymouth, UK

[c]Engineering and the Environment, University of Southampton, UK

[d]Seabased AB, Uppsala, Sweden

ABSTRACT

The survivability of a 1:20 scale point-absorbing wave energy converter model is considered in extreme wave tests with focused waves embedded in regular wave backgrounds, as well as with time-series of irregular waves. The wave heights were many times higher than the maximal stroke length of the device. Three different float geometries have been used in the tests. Peak loads are measured and compared for extreme waves embedded in background waves with a range of periods and phase relations and different values of power-take off damping.

KEY WORDS: wave energy, extreme waves, tank tests, power take-off damping, maximum forces, survivability.

INTRODUCTION

One of the most challenging problems for wave energy to be an economically viable energy source is to ensure reliable energy production and survivability also in extreme weather conditions outside the normal operational wave climates.

Extreme waves are rare, but when they occur, they can lead to large structural damages on the off-shore structure, may it be a platform, ship or a wave energy converter. Extreme waves are surface gravity waves whose wave heights are much larger than expected for the sea state. They are characterized by a high crest between two deep troughs. Some studies indicate that extreme wave events are more common than previously thought (Dysthe, Krogstad and Muller 2008), and that their rate of occurrence is increasing (Ruggiero, Komar and Allan, 2010).

In ocean engineering, the impact of high and steep waves has been a subject of research for many decades (Molin 1979; Mei 1983; Lighthill 1986; Eatock-Taylor and Hung 1987). Different approaches to model the non-linear behavior of steep waves include semi-empirical methods, non-linear potential flow methods, full CFD-methods, or combinations of these. However, CFD-modelling is very computationally demanding, and all the numerical models still depend on physical experiments for validation. The impact of extreme waves is also highly depending on the off-shore structure in question.

Physical experiments of wave loads on truncated vertical cylinders were reported by Ransley, Hann, Greaves and Simmons (2013) and the results compared with numerical simulations with OpenFOAM with good agreement. For the point-absorbing wave energy converters Wavestar, physical tank tests were compared with computations of Froude-Krylov forces and linear diffraction theory by Viuff, Andersen, Kramer and Jakobsen (2013).

Here, we present experimental results of the forces of high, steep but non-breaking waves on point-absorbing wave energy devices. The buoy is freely floating but attached to a linear power take-off (PTO) model with limited stroke-length. Both focused waves embedded in regular wave backgrounds and irregular waves are studied, and the wave heights are several times the maximal stroke length of the device. In particular, this paper analyses how the wave height of the individual waves affects the force peaks, and the variability of the wave loads. In order to provide quick estimates and guidelines for developers of wave energy technologies, all set-up dimensions and the results will be presented in full-scale values.

METHOD

Model

Using Froude scaling, a 1:20 scale model has been constructed based on the point-absorbing wave energy converter (WEC) developed at Uppsala University, Sweden. The dimensions of the model and the corresponding full-scale values are presented in Table 1 and can be seen in Fig. 1. The model consists of a float connected through a line and pulley system to a power take-off model situated on a gantry above the water level. The power take-off damping is modelled physically by a friction damping, applied by adjustable Teflon blocks pressing against the “translator” that is moving vertically in the power take-off model.

Table 1. Dimensions of the model and the corresponding dimensions in the full-scale WEC. The PTO damping values are only approximate.

	1:1 full-scale	1:20 model
Buoy outer/inner radius CM and CWD	2 m / 1.03 m	0.1 m / 0.052 m
Buoy radius CYL	1.7 m	0.085 m
Buoy draft CM, CWD	0.94 m	0.047 m
Buoy draft CYL	0.64 m	0.032 m
Translator stroke length	4.4 m	0.22 m
Buoy mass CWD	8.6 tons	1.07 kg
Buoy mass CM	7.2 tons	0.90 kg
Buoy mass CYL	5.7 tons	0.72 m
Translator mass	6.24 tons	0.780 kg
Spring constant	776 kN/m	1.94 kN/m
PTO damping 1	~18 kN	~2.25 N
PTO damping 2	~59 kN	~7.38 N
PTO damping 3	~83 kN	~10.4 N
Water depth	50 m	2.5 m

The force which the friction break exerts on the moving translator is given in units N in Table 1. For a full-scale device, this corresponds to an electric damping in the generator at a constant translator speed. At the top-end, the translator movement is damped by an end-stop spring, which is the case also in the full-scale WEC, as can be seen in Fig. 1.

Several different documents with guidelines for WEC survivability experiments have been published. Holmes and Nielsen (2010) suggest that tests should be performed both at small scale (1:100 up to 1:25) and medium scale (1:25 up to 1:10). Here, a 1:20 scale has been chosen as a compromise between large enough scale to neglect friction and viscous effects, and small enough scale to be able to generate the correct amplitude of extreme waves in the wave tank.

Three different floats have been used in the experiments: a cylinder float (CYL), a cylinder float with a moonpool (CM) and a cylinder float with a moonpool and additional water damping (CWD). The floats can be seen in Fig. 1; the float with moonpool and no additional water damping is obtained by removing the top "hat" of the leftmost float in the picture. The attachment point of the line to the power take-off is centered on the vertical axis for all floats.

Extreme Waves Events

Extreme wave events are typically derived from site-specific historical wind and wave data, from which a return period of extreme waves can be statistically determined. Common return periods for off-shore structures survivability design is 100 years, but Coe and Neary (2014) suggest that an appropriate design criterion for WEC survivability is return periods of 50 years. For these experiments, an 80-year return period sea state at the Wave Hub site has been chosen. The Wave Hub is located in the south-west UK and constitutes one of the most energetic wave climate sites in Europe. At the 1:20 scale chosen for the experiments, the wave height of the 80-year return period extreme wave can be correctly reproduced in the wave basin using NewWave theory (Tromans, Anaturk and Hagemeier, 1991), but the wave shape is slightly steeper.

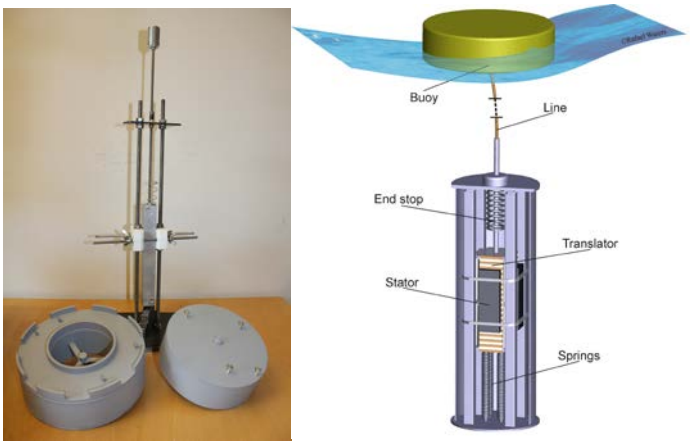

Fig 1. The model used in the experiments, and an illustration of the full-scale WEC. The full-scale PTO damping is electrical, whereas in the model it is asserted by friction brakes acting on the translator.

All waves in the experiments are monodirectional, with negligible wave reflection from the sides of the wave basin. The extreme wave generation is described more in detail by Ransley, Hann, Greaves, Raby and Simmonds (2013).

Embedded Focused Waves. In the experiments, focused waves embedded in regular wave backgrounds were used. The focused waves were embedded into different phase positions within the regular wave. In total, 32 different embedded focused waves were used, divided in four sets with background period 10 s, 10.7 s, 12.7 s and 13.7 s. The regular background wave height was 7.2 m for all tests. Each of the four sets contained eight tests where the phase position for the embedding within the regular wave was $\pi(k-1)/4$, with $k=1,\ldots,8$. Here, the focused wave tests are labelled T_{jk}, where $j=1,\ldots4$ represents the different background periods. The embedded focused waves were chosen so as to provide a more controlled experiment of extreme wave events, and to study the wave load and the response of the float from the extreme wave in different background embedding.

Irregular Waves. To provide more realistic conditions, experiments with time-series of extreme irregular waves were also conducted. For off-shore structures with constrained motions, such as a wave energy converter with fixed mooring or stroke length, also non-extreme but high waves may cause high forces and fatigue or damage to the structure, and a number of factors are likely to influence the device response to the waves. Whereas the embedded focused wave tests will provide information on maximum force as function of one incoming extreme wave with determined wave height, the irregular wave tests measure the wave loads in a more unpredictable setting.

Two different time-series of irregular waves were used, referred to here as I_1 and I_2. Their spectrum is generated using standard JONSWAP spectra and they differ in the significant wave height $H_s^{(1)}$ = 7.4 m, $H_s^{(2)}$ = 7.2 m, and in their energy period $T_e^{(1)}$ = 12.9 s, $T_e^{(2)}$ = 11.7 s. The time-series of each irregular wave test is recorded for 67 minutes each (corresponding to 15 min in 1:20 scale).

Experiments

The experiments were conducted at the COAST Laboratory of Plymouth University, UK. The wave tank measures 35 x 15.5 m, has raiseable floor and is equipped with 24 flap-type paddles. The surface

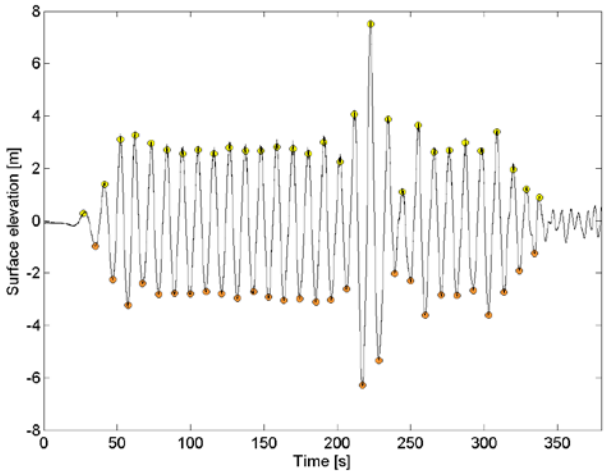

Fig 2. Surface elevation measured at the float for the embedded focused wave test T_{11}, with corresponding force measurements shown in Fig. 3.

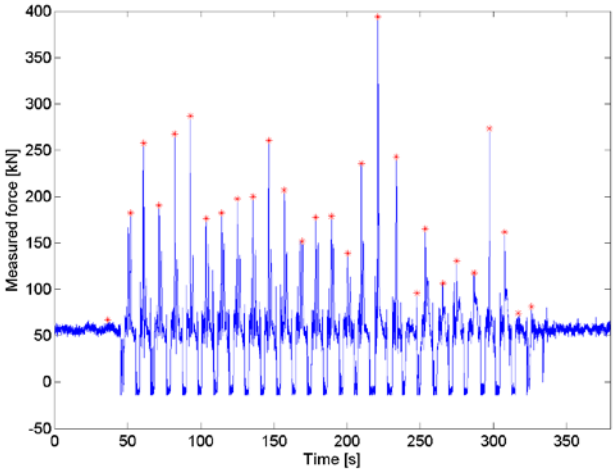

Fig 3. Force measurements for the embedded focused wave test T_{11}, corresponding to the embedded focused wave data in Fig. 2.

elevation was measured with a set of calibrated resistive wave gauges. The force in the line was measured by a miniature low profile load cell, attached to the top of the translator and connected to the buoy through a non-elastic line. The mass of the load cell is 0.45 kg and is included in the full mass of the translator in Table 1.

The position of the buoy was measured with the optical Qualisys system, consisting of 5 cameras placed outside the basin and 4 infrared reflecting markers attached by rods on the buoy. The load cell and the motion capture system were synchronized and had a sampling frequency of 128 Hz.

RESULTS

Extreme Forces as Function of Wave Height

Embedded Focused Waves. For each of the 32 focused waves imbedded in regular waves, the incoming waves have been measured at a wave gauge close to the buoy. The wave peaks and troughs in each test have been identified as shown in Fig. 2. From the figure, it is clear that the focused wave hits at 224 s and that the remaining test cycle is comprised of regular waves of roughly the same height.

Each incoming wave is then correlated with the corresponding force measurement of the same test, as plotted in Fig. 3. More specifically, the maximal force in the time interval between two adjacent wave troughs have been identified and is marked in Fig. 3 with a red asterisk. Already from the Fig. 3, it is clear that the magnitude of the force peaks varies even in the regular wave background before the focused wave hits. For the test T_{11} plotted in Fig. 2-3, there are in total 29 wave troughs and corresponding 28 identified force peaks.

This has been repeated in a systematical way for all the 32 embedded focused wave tests. Depending on the background wave period, the amount of force peaks in each tests ranges from 22 to 28. For each individual wave, the wave height has been determined as the vertical distance from the preceding wave trough to the wave peak.

Negative large forces have been measured when the translator hits the lower end-stop with full speed. In a full-scale WEC, the motion will be damped, and these negative peaks have been omitted here.

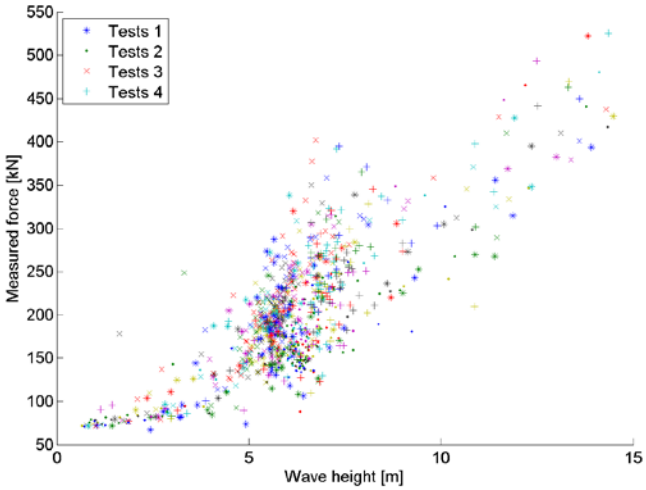

Fig 4. Force peaks in all 32 tests with focused waves embedded in regular wave backgrounds. In each tests, 22-28 force peaks have been identified and are plotted. The accumulation of data points in the wave height range 5-7 m correspond to the regular wave background.

All force peaks are plotted against the wave height of the corresponding wave in Fig. 4; Tests T_{jk} with $j=1$ have background period 10.7 s and are plotted with asterisks (*), tests with $j=2$ have background period 12.7 s and are plotted with points (.), tests $j=3$ have background period 13.7 s and are plotted with crosses (x), and finally tests $j=4$ have background period 10.0 s and are plotted with pluses (+). The individual tests $k=1,\ldots,8$ are indicated with different colors, but will not be investigated in any detail here. All tests in Fig. 4 are performed for the cylinder float with moonpool and water damping (CWD).

As is clear from Fig. 4, the measured force follows a clear trend as a function of the wave height, with an accumulation of force peaks in the range 100-350 kN for wave heights 5-7 m, which is the regular wave background. The highest measured forces are obtained for the largest wave heights > 12 m. Still, despite the small variability in the wave height of the incoming waves, the variability in the measured force peaks is rather large. Corresponding scatter diagram in the case of nonzero PTO damping values is shown in Fig. 9.

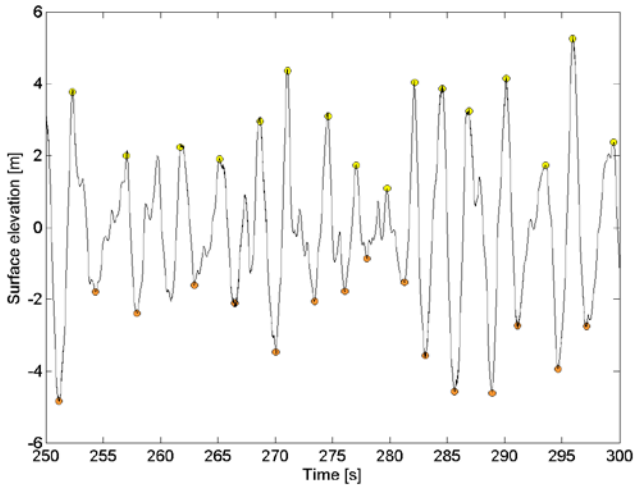

Fig 5. Surface elevation for the irregular wave test I_2 as detected by a wave gauge in the direct vicinity of the cylinder (CYL) float.

Irregular Waves. The identification of the peaks and troughs in the irregular waves is not as straight-forward as for the embedded focused wave tests discussed above. Fig. 5 shows the surface elevation for a time period of 50 s and illustrates this. Unlike the regular waves in Fig. 2, we are not interested in *all* local wave peaks and troughs, but instead of the waves with a large vertical trough-to-peak distance. Hence, in the algorithm to determine the troughs and peaks, each peak is defined as the global maximum within 13.9 s from the previous peak, implying that some local wave maximums and minimums have been neglected, as can be seen in Fig. 5. The rest of the time spectrum for the irregular wave tests (in total 67 min) looks similar, with almost all major troughs and peaks detected, but some local extremes ignored. After the peaks and troughs in the irregular wave tests have been identified, the corresponding maximum force between each pair of succeeding wave troughs have been detected. The measured force together with the identified peak forces is shown in Fig 6, corresponding to the same test and time period as in Fig. 5.

The force peaks are plotted against the wave height for each individual wave in Fig. 7, where the wave height is again computed as the vertical distance from the preceding trough to the wave peak.

Irregular wave test I_1 for the cylinder float (CYL) is plotted with red asterisks and test I_2 for same float with black pluses. For both irregular wave tests, 268 force events have been identified and plotted. The equivalent scatter diagram of the cylinder with moonpool float (CM) can be seen in Fig. 8, both for the case with and without PTO damping.

As can be seen in Fig. 7, there is a large variability of the detected maximum forces for the same wave height. A similar large variability in the total force as function of the wave crest elevation has been reported for extreme wave tests on vertical cylinders by Chaplin and Rainey (2012).

Extreme Forces as Function of PTO Damping

The WEC model in these experiments is equipped with a simple power take-off damping consisting of Teflon blocks asserting friction brakes on the translator motion. All results presented in Fig. 2-7 refer to experiments performed with zero PTO damping. To investigate the influence of PTO damping, Fig. 8 compares irregular wave tests with and without damping and clearly shows that the PTO damping reduces

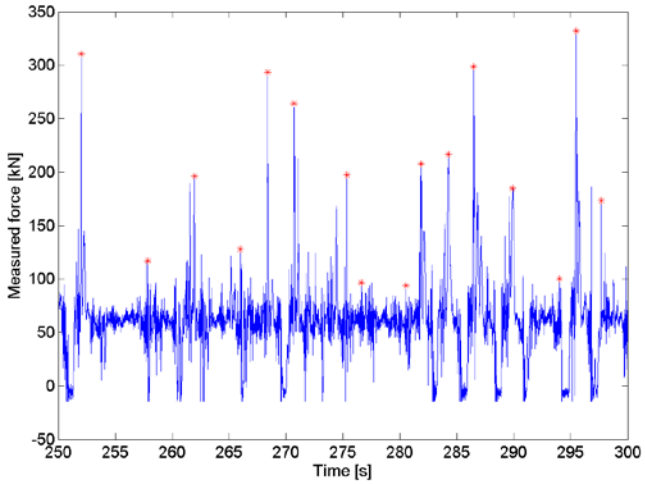

Fig 6. Force measurements for the irregular wave tests I_2 for the cylinder float (CYL), as well as the identified force corresponding to each individual wave in Fig. 5.

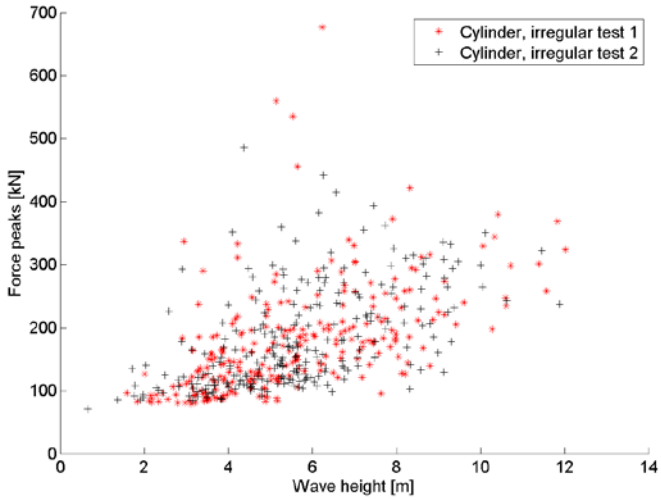

Fig 7. Measured force peaks in irregular wave tests I_1 and I_2 for the cylinder float (CYL), plotted against the individual wave height of the incident wave.

the force measured in the line between the float and the translator.

Similarly, in Fig. 9, one of the embedded focused wave test T_{12} has been plotted for the three cases with PTO damping 18 kN, 59 kN and 83 kN. When comparing Fig. 4 and 9, one observes that the damped cases (Fig. 9) display lower measured force peaks and that the variability in the measured forces is reduced. The mean of the maximal force obtained in each of the 32 tests without PTO damping in Fig. 4 is 410 kN. The corresponding mean values for the maximal force obtained in each of the test in Fig. 9 is 379 kN, 280 kN and 187 kN, respectively for the three increasing PTO damping values.

Finally, to complete the picture of the influence of the PTO damping, the corresponding time-series of measured force peaks in the three tests T_{12} with PTO damping have been plotted in Fig. 10. In these tests, the embedded focused wave hits the float at t = 134 s. In the leftmost plot, a weak PTO damping of ~18 kN is used, and the variability in the force peaks are similar to that of the undamped test in Fig. 3.

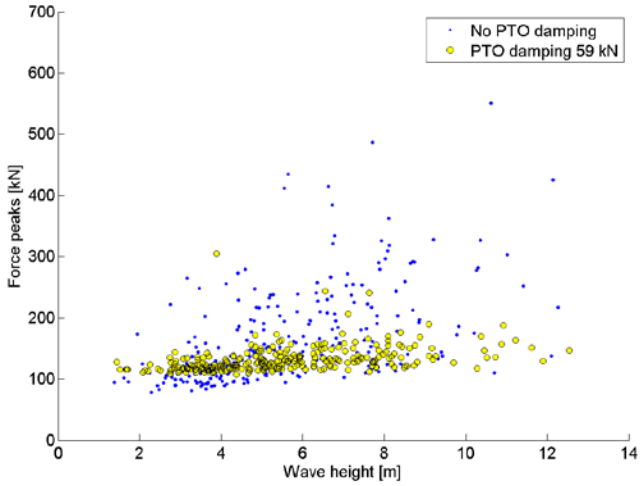

Fig 8. Measured force peaks in irregular wave tests I_1 for the cylinder with moonpool float (CM), plotted against the individual wave height of the incident wave.

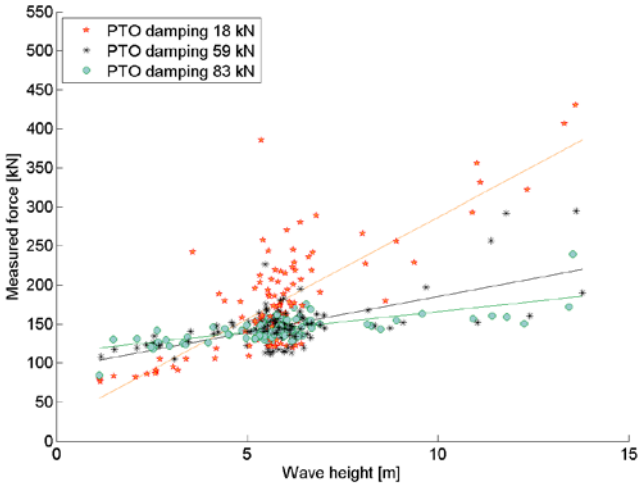

Fig 9. Measured force peaks in the embedded focused wave test T12 for the CWD float with the three different values of PTO damping. Linear trend lines have been added for visibility. Compare with Fig. 4 for the case without PTO damping.

As the magnitude of the PTO damping increases to ~59 kN in the middle plot, the force peaks are effectively reduced, and in the overdamped system in the rightmost plot, there is no visible force peak due to the embedded focused wave.

Response of Different Floats in Extreme Waves

Three different floats were used in the tank tests. When comparing the irregular wave test I_1 without damping in Fig. 7 and 8, a slight tendency for higher force peaks for the cylinder (Fig. 7) than for the CM float (Fig. 8) can be perceived.

DISCUSSION

Both the embedded focused waves and the irregular waves conducted in these experiments were non-breaking and mono-directional with negligible reflections from the sides of the wave basin. It can be expected that the wave loads will decrease somewhat in omnidirectional waves (Parmeggiani, Kofoed and Friis-Madsen, 2011).

The results in Fig. 2-7 show that the variability in the measured forces is very big. In the irregular wave tests, a certain amount variability is expected, but the obtained variability in the measured force even in the regular wave background of the focused wave in Fig. 3-4 is somewhat surprising. By comparing the regular wave background in Fig. 2 and the corresponding force peaks in Fig. 3, the large variability can be quantified: the normalized standard deviation of the regular wave heights during the time interval 50-190 s in Fig. 2 is only 0.08, but the normalized standard deviation of the corresponding force peaks during the same time in Fig. 3 is 0.2, i.e. 2.6 times higher. Also, the variability in the measured forces in the irregular waves in Fig. 6-7 is larger than anticipated.

Not only the wave height but rather the steepness of the individual waves will affect the motion of the float and the wave loads on the device. Although, in general, wave loads are expected to grow with wave height, there are possibly a number of local force maximums associated with certain wave periods and height combinations (Coe and Neary, 2014), corresponding to points of resonance, for instance.

In the regular wave backgrounds used for the embedded focused wave tests, four different values for the wave period have been used, and the irregular wave tests contain a large spectrum of waves with different steepness. This may explain some of the variability in the force measurements between different tests and in the irregular tests, but it still doesn't explain the variability in the background regular waves, see Fig. 3.

Many factors may influence the wave loads on the device. For example, the position of the float at the instant when the wave hits will possibly affect the measured forces. Even for the controlled experiments with regular waves, small deviations in the position due to the previous waves may influence the device response to the waves, and thereby affect the measured forces.

Despite the choice of 1:20 scale, there is undoubtedly friction and viscosity present in the experiments, which adds to the uncertainties of the results. Another source of uncertainty in the experiments is the existence of the end-stop spring. The scale model was designed with an end-stop to resemble the full-scale wave energy device, where an end-stop spring is used to damp the largest vertical motions of the translator and prevent damage to the generator hull or mooring lines during high waves. The magnitude of the spring force in the model was chosen so as to contract partly during the extreme wave tests, but never to be fully contracted. The same spring has been used throughout the experiments. In each wave cycle, the spring was retracted to its full length, hence a priori, the velocity of the float in waves of equal wave height should be exposed to the same force by the spring. Nevertheless, the spring was not completely fixed in a vertical position, and could potentially have contracted differently in different wave cycles due to small differences in its position and the stiffness of the spring, which could possibly have influenced the measured forces. In future experiments, controlled tests without and with different end-stop springs (possibly longer and with less stiffness) would be interesting.

Fig. 8-10 show measured force peaks in experiments with and without PTO damping. The figures demonstrate how the force peaks reduce when the PTO damping is increased. The variability of the measured force peaks is reduced when a PTO damping is applied, which can be seen in Fig. 9-10. The normalized variance of the peaks in the three

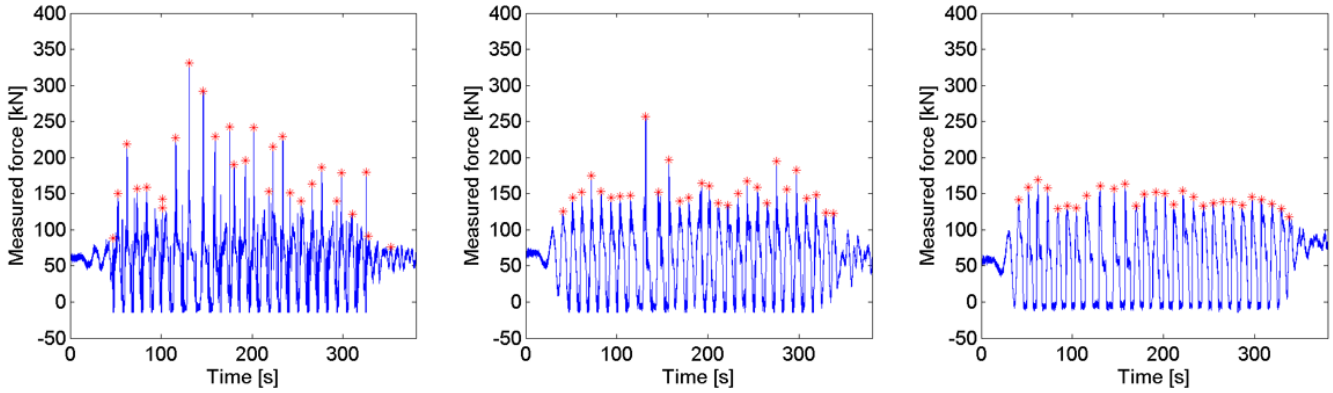

Fig 10. Force measurements for the embedded focused wave test T_{12} with three different (approximate) values of the PTO damping: 18 kN (left), 59 kN (middle) and 83 kN (right).

tests with increasing damping in Fig. 10 is 0.11, 0.031 and 0.0073, respectively.

Even in the case with PTO damping, there is a tendency for increased wave load with higher wave heights, as can be seen in Fig. 9, but the slope decreases and is almost flat for the overdamped system with the highest PTO damping.

CONCLUSIONS

A 1:20 scale model of a point-absorbing wave energy converter has been subjected to extreme wave tests using both focused waves embedded in a regular wave background, and time-series of irregular waves. The force in the line connecting the buoy and the generator has been measured and the force peaks have been matched with the corresponding incident waves. This has enabled an analysis of the force peaks as function of the individual wave height of the incident extreme waves.

Our results show that the variability in the measured force peaks is large, even in the regular background waves with roughly the same wave heights. In the irregular wave tests, the scattering among the force peaks is even larger. An applied PTO damping to the model not only reduces the average magnitude, but also reduces the variability of the measured peak forces.

ACKNOWLEDGEMENTS

This research is supported by StandUp for Energy, Uppsala University, Carl Tryggers Stiftelse, the Swedish Energy Agency, Bengt Ingeströms scholarship fund, the Wallenius foundation, and Miljöfonden.

REFERENCES

Chaplin, JR and Rainey, RCT (2012). “Long-duration experiments in irregular waves, to determine 10 000-year wave loads on a 3.5 m diameter vertical cylinder”, in *Proc. if the International Workshop for Water Waves and Floating Bodies (IWWWFB)*, Copenhagen, Denmark.

Coe, RG and Neary, VS (2014). “Review of methods for modeling wave energy converter survival in extreme sea states”, in *Proc. of the 2nd Marine Energy Technology Symposium (METS)*, Seattle, USA.

Dysthe, K, Krogstad, H and Müller, P (2008). ”Oceanic rogue waves”, *Annual Review of Fluid Mechanics* 40, 287–310.

Eatock Taylor, R and Hung, S (1987). “Second-order diffraction forces on a vertical cylinder in regular waves”, *Applied Ocean Research* 9, 19–30.

Engström, J, Göteman, M, Eriksson, M, Hann, M, Ransley, E, Greaves D and Leijon M (2015). ”Scale tests on the survivability of point-absorbing wave energy converters–part II,” *submitted to Journal of Renewable Energy*.

Holmes, B and Nielsen, K (2010). “Guidelines for the development & testing of wave energy systems”, Tech. Rep. T02-2.1, *Ocean Energy Systems (OES)*.

Lighthill, J (1986). “Fundamentals concerning wave loading on offshore structures”, *J. Fluid Mech.* 173, 667.

Mei, C (1983). “The Applied Dynamics of Ocean Surface Waves”, Wiley.

Molin, B (1979). “Second-order diffraction loads upon three-dimensional bodies”, *Appl. Ocean Res.* 1, 197.

Parmeggiani, S, Kofoed, J and Friis-Madsen, E (2011). “Extreme loads on the mooring lines and survivability mode for the wave dragon wave energy converter”, in *Proc. of the World Renewable Congress*, Linköping, Sweden.

Ransley, E, Hann, M, Greaves, D, Raby, A, and Simmonds, D (2013). “Numerical and physical modelling of extreme wave impacts on a fixed truncated circular cylinder”, in *Proc. of the 10th EWTEC conference*, Aalborg, Denmark.

Ruggiero, P, Komar, P and Allan, J (2010). ”Increasing wave heights and extreme value projections: The wave climate of the US Pacific Northwest”, *Coastal Engineering* 57(5), 539–552.

Tromans, P, Anaturk, A and Hagemeier, P (1991). “A new model for the kinematics of large ocean waves – application as a design wave”, in *Proc. of the 1st International Offshore and Polar Engineering Conference*, Edinburgh, Scotland.

Viuff, T, Andersen, M, Kramer, M and Jakobsen, M (2013). ”Excitation forces on point absorbers exposed to high order non-linear waves”, in *Proc. of the 10th EWTEC conference*, Aalborg, Denmark.